JOURNAL OF COMPUTATIONAL PHYSICS **128,** 319–330 (1996)
ARTICLE NO. 0213

Computations of Boundary Optimal Control Problems for an Electrically Conducting Fluid

L. S. HOU*,[1] AND S. S. RAVINDRAN†,[2]

*Department of Mathematics and Statistics, York University, North York, Ontario, M3J 1P3, Canada; †Center for Research in Scientific Computation, Department of Mathematics, North Carolina State University, Raleigh, North Carolina 27695-8205

Received June 12, 1995; revised February 14, 1996

We study four optimal control problems for an electrically conducting fluid. The control is the (normal) electrical current on the boundary of the flow domain. The objectives are to match a desired velocity field, or to match a desired electrical potential field, or to minimize the potential gradient, or to minimize the vorticity in the flow domain. We develop a systematic way to use the Lagrange multiplier rules to derive an optimality system of equations from which an optimal solution can be computed. Mixed finite element methods are used to find approximate solutions for the optimality systems of equations that characterize the optimal controls. A direct method and an iterative method are proposed for solving the discrete, nonlinear optimality systems of equations. Numerical results for several examples are presented.

1. INTRODUCTION

The control of electrically conducting flows for the purpose of achieving some desired objective is crucial to many technological applications such as fusion technology, design of novel submarine propulsion devices, and modeling of nuclear reactors or molten metal string. In this paper we study four control problems for a steady, electrically conducting fluid. We cast these problems as constrained optimization problems, namely that of computing the electric current on the flow boundary that minimizes appropriate cost functional relevant to the physics of the flow. The first problem involves driving the fluid velocity $\mathbf{u}$ to a desired velocity $\mathbf{u}_d$ in the flow domain. The second and third one involves, respectively, matching the electric potential ϕ to a desired one or minimizing the potential gradient in the flow region. The fourth one is motivated by the fact that irrotational flows incur low energy dissipation; therefore we consider the minimization of total vorticity in the flow.

Subject classification 65N30, 49K20, 76W05, 76D05.

[1] The work of this author is supported in part by Natural Science and Engineering Research Council of Canada under Grant OGP-0137436 and by a York University Faculty of Arts Research Grant.

[2] The work of this author is supported in part by AFOSR F49620-93-1-0355.

The methods proposed in this paper are applicable to more general optimal control problems in viscous incompressible flows with various types of controls than the particular problems studied in this paper.

Optimal control and optimization for MHD flows have been the subject of extensive research in the literature. Most notably there are well-established bodies of literature on optimization of liquid-metal MHD in the following areas: the optimal choice of positions and electric currents for AC induction coils in order to achieve a desired free-surface shape in electromagnetic levitation of liquid-metal droplets; the optimal positioning of AC coils and magnetic shields in the continuous casting of aluminum and other metals in order to achieve the melt flow free-surface stability needed for optimum solid structure; the shaping of a nonuniform magnetic field applied during the growth of semiconductor crystals in order to achieve uniform crystal properties and the design of fusion reactor cooling systems by properly choosing the geometry and conductivity of the ducts in order to optimize the thermalhydraulic performance of the reactor. However, as far as we know, only recently did scientists and mathematicians began to study *rigorously* such mathematical properties as the existence and smoothness of optimal solutions, the existence of Lagrange multipliers when the Lagrange multiplier approach is used, and the convergence and error estimates for various approximation methods used to find optimal solutions; some of these mathematical results can be found in, e.g., [1, 4–6]. Reference [1] contains both rigorous and formal mathematical proofs and lists many open (mathematical) problems, some of which still remain open. Despite the lack of rigorous mathematical proofs and justifications for every detail, scientists and engineers have, as mentioned previously, applied successfully various optimization techniques to solve practical optimal control problems in MHD. Various numerical methods have been developed. The purpose of this article is: first, to develop a systematic (formal) procedure for solving numerically optimal control problems for MHD flows—this formal procedure we hope is easier to follow by nonspecialists; second, to establish

0021-9991/96 $18.00

some test examples for optimal control of MHD flows; and third, to demonstrate the effectiveness of optimal control and some numerical methods. Rigorous error estimates for the numerical methods used in this paper will be presented elsewhere; see [6] and forthcoming work by the authors. We also point out that, although the numerical examples presented in this article are mostly of an academic nature, they serve the purpose of demonstrating the possible applications of the optimal control methods in more complicated, industrial situations.

We now give an outline for the rest of the paper. In the remainder of this section, we will first describe the governing equations and boundary conditions for the type of electrical conducting fluid that we will deal with and then state the optimal control problems that we will study. In Section 2, we introduce a variational formulation of the constraint equations; we then develop a systematic way of using Lagrange multiplier rules to derive an optimality system of equations for the constrained minimization problem. In Section 3, we define finite element approximations of the optimality system of equations. In Section 4, we discuss solution techniques for the optimality system. In Section 5, we summarize useful mathematical results and error estimation results. In Section 6, some numerical results are presented. Finally in Section 7, we make some brief concluding remarks.

1.1. *Governing Equations for an Electrically Conducting Fluid*

The dimensionless equations governing the steady incompressible flow of an electrically conducting fluid in the presence of a magnetic field are given by

$$\frac{1}{N}(\mathbf{u}\cdot\nabla)\mathbf{u} = -\nabla p + (\mathbf{j}\times\mathbf{B}) + \frac{1}{M^2}\Delta\mathbf{u} + \mathbf{f} \quad \text{in } \Omega,$$

$$\nabla\cdot\mathbf{u} = 0 \quad \text{in } \Omega,$$

$$\mathbf{j} = -\nabla\phi + (\mathbf{u}\times\mathbf{B}) \quad \text{in } \Omega,$$

$$\nabla\cdot\mathbf{j} = 0 \quad \text{in } \Omega,$$

$$\nabla\times\mathbf{B} = R_{\mathrm{m}}\mathbf{j} \quad \text{in } \Omega,$$

$$\nabla\cdot\mathbf{B} = 0 \quad \text{in } \Omega,$$

where $\mathbf{u}$ denotes the velocity field, p is the pressure field, $\mathbf{j}$ is the electric current density, $\mathbf{B}$ is the magnetic field, and ϕ is the electric potential. Also, N is the interaction number, M is the Hartmann number,and R_{m} is the magnetic Reynolds number. We denote by Ω the flow domain which is a bounded open set in $\mathbb{R}^2$ or $\mathbb{R}^3$ with a boundary Γ.

Although the problems and the methods to be studied in this paper are applicable to the optimal control for general models of magnetohydrodynamic flows, purely for the simplicity of explaining the ideas, we will deal with a special case in which the externally applied magnetic field is undisturbed by the flows. In particular, we assume that $\mathbf{B}$ is given. Such an assumption can be met in a variety of physical applications, e.g., in the modeling of electromagnetic pumps and the flow of liquid lithium for fusion reactor cooling blankets [12, 13].

Note that if the flow is two-dimensional, our convention in this paper is that the applied magnetic field $\mathbf{B}$ is perpendicular to the flow plane, i.e., $\mathbf{B} = (0, 0, B(x, y))^{\mathrm{T}}$, and that the cross product $\mathbf{u}\times\mathbf{B}$ is understood as $(u_1, u_2, 0)^{\mathrm{T}} \times (0, 0, B(x, y))^{\mathrm{T}}$.

By eliminating $\mathbf{j}$ we arrive at the following simplified system (see [8]):

$$-\frac{1}{M^2}\Delta\mathbf{u} + \frac{1}{N}(\mathbf{u}\cdot\nabla)\mathbf{u} + \nabla p - (\mathbf{B}\times\nabla\phi) - (\mathbf{u}\times\mathbf{B})\times\mathbf{B} = \mathbf{f} \quad \text{in } \Omega, \tag{1.1}$$

$$\nabla\cdot\mathbf{u} = 0 \quad \text{in } \Omega, \tag{1.2}$$

and

$$-\Delta\phi + \nabla\cdot(\mathbf{u}\times\mathbf{B}) = 0 \quad \text{in } \Omega. \tag{1.3}$$

In (1.1)–(1.3), $\mathbf{B}$ and $\mathbf{f}$ are given data.

The system (1.1)–(1.3) is supplemented with boundary conditions

$$\mathbf{u} = \mathbf{0} \quad \text{on } \Gamma \tag{1.4}$$

and

$$\frac{\partial\phi}{\partial n} = g \quad \text{on } \Gamma, \tag{1.5}$$

where g denotes the only control variable, namely, the normal electric current on Γ. Such a control can be effected by attaching electric sources with adjustable resistors to the electrode along the flow boundary. Although a normal electric current control is physically somewhat artificial (this could be achieved in practice only by insulating different small parts of an electrode from each other), it is mathematically more convenient than an electrical potential control. The techniques to treat normal electric current controls are applicable to treat other types of controls; and the solutions with a normal electric current control do indicate the behavior to expect in general. See [7] for the use of this type of boundary conditions.

1.2. *Optimal Control Problems*

Our goal is to try to obtain a desired flow field by appropriately choosing the control—the normal electric current on Γ. Specifically we will investigate the following cases:

matching a desired velocity field, matching a desired potential field, minimizing the potential gradient, or minimizing the vorticity. Mathematically, these tasks can be described, respectively, by the following optimal control setting: minimize the cost functional

$$\mathscr{K}(\mathbf{u}, \phi, p, g) = \frac{1}{2\varepsilon}\int_\Omega |\mathbf{u} - \mathbf{u}_d|^2\, d\Omega + \frac{\delta}{2}\int_\Gamma |g|^2\, d\Gamma, \quad (1.6)$$

or

$$\mathscr{M}(\mathbf{u}, \phi, p, g) = \frac{1}{2\varepsilon}\int_\Omega |\phi - \phi_d|^2\, d\Omega + \frac{\delta}{2}\int_\Gamma |g|^2\, d\Gamma, \quad (1.7)$$

or

$$\mathscr{N}(\mathbf{u}, \phi, p, g) = \frac{1}{2\varepsilon}\int_\Omega |\nabla\phi|^2\, d\Omega + \frac{\delta}{2}\int_\Gamma |g|^2\, d\Gamma, \quad (1.8)$$

or

$$\mathscr{V}(\mathbf{u}, \phi, p, g) = \frac{1}{2\varepsilon}\int_\Omega |\operatorname{curl}\mathbf{u}|^2\, d\Omega + \frac{\delta}{2}\int_\Gamma |g|^2\, d\Gamma, \quad (1.9)$$

subject to the constraints (1.1)–(1.5). Here $\varepsilon > 0$ and $\delta > 0$ are positive parameters that adjust the relative weight of the two terms in the functional; $\mathbf{u}_d$ and ϕ_d are, respectively, desired velocity field and potential field.

The minimization of functionals (1.6), (1.7), (1.8), or (1.9) subject to (1.1)–(1.5) is the special case of the general optimal control setting

$$\begin{aligned}&\text{minimize the cost functional } \mathscr{I}(\mathbf{u}, \phi, p, g)\\ &\quad = \mathscr{F}(\mathbf{u}, \phi, p) + \frac{\delta}{2}\int_\Gamma |g|^2\, d\Gamma, \qquad (1.10)\\ &\text{subject to the constraints (1.1)–(1.5),}\end{aligned}$$

where $\mathscr{F}(\mathbf{u}, \phi, p)$ is a functional of $(\mathbf{u}, \phi, p)$.

2. A VARIATIONAL FORMULATION OF THE CONSTRAINTS; AN OPTIMALITY SYSTEM OF EQUATIONS

The first step in our systematic procedure involves rewriting the governing flow equations (for the special case of the electrically conducting fluid mentioned previously) in a variational form. To this end, we introduce the function space $H^1(\Omega) = \{v \in L^2(\Omega) : \partial v/\partial x_i \in L^2(\Omega) \text{ for } i = 1, ..., d\}$, where $d = 2$ or 3; $H_0^1(\Omega) = \{v \in H^1(\Omega) : v|_\Gamma = 0\}$; $L_0^2(\Omega) = \{q \in L^2(\Omega) : \int_\Omega q\, d\Omega = 0\}$; $\tilde{H}^1(\Omega) = H^1(\Omega) \cap L_0^2(\Omega)$; and $H^m(\Omega) = \{v \in L^2(\Omega) : \partial^{|\alpha|} v/\partial x_1^{\alpha_1} \cdots \partial x_d^{\alpha_d} \in L^2(\Omega), \text{ for all } \alpha = (\alpha_1, ..., \alpha_d) \text{ with } |\alpha| \le m\}$. Vector-valued counterparts of these spaces are denoted by boldface symbols, e.g., $\mathbf{H}^1(\Omega) = [H^1(\Omega)]^d$.

The variational formulation of the constraint equations is then given as

$$\begin{aligned}&\text{seek } \mathbf{u} \in \mathbf{H}_0^1(\Omega), p \in L_0^2(\Omega), \text{ and } \phi \in \tilde{H}^1(\Omega) \text{ such that}\\ &\frac{1}{M^2}\int_\Omega \nabla\mathbf{u} : \nabla\mathbf{v}\, d\Omega + \int_\Omega [\nabla\phi - (\mathbf{u}\times\mathbf{B})]\cdot[\nabla\psi - (\mathbf{v}\times\mathbf{B})]\, d\Omega\\ &\quad + \frac{1}{N}\int_\Omega (\mathbf{u}\cdot\nabla)\mathbf{u}\cdot\mathbf{v}\, d\Omega - \int_\Omega p\nabla\cdot\mathbf{v}\, d\Omega \qquad (2.1)\\ &\quad = \int_\Omega \mathbf{f}\cdot\mathbf{v}\, d\Omega + \int_\Gamma g\psi\, d\Gamma \quad \forall(\mathbf{v}, \psi) \in \mathbf{H}_0^1(\Omega)\times\tilde{H}^1(\Omega)\end{aligned}$$

and

$$\int_\Omega q\nabla\cdot\mathbf{u}\, d\Omega = 0 \quad \forall q \in L_0^2(\Omega), \qquad (2.2)$$

or, equivalently, seek $\mathbf{u} \in \mathbf{H}_0^1(\Omega)$, $p \in L_0^2(\Omega)$, and $\phi \in \tilde{H}^1(\Omega)$ such that

$$\begin{aligned}&\frac{1}{M^2}\int_\Omega \nabla\mathbf{u} : \nabla\mathbf{v}\, d\Omega - \int_\Omega [\nabla\phi - (\mathbf{u}\times\mathbf{B})]\cdot(\mathbf{v}\times\mathbf{B})\, d\Omega\\ &\quad + \frac{1}{N}\int_\Omega (\mathbf{u}\cdot\nabla)\mathbf{u}\cdot\mathbf{v}\, d\Omega \qquad (2.3)\\ &\quad - \int_\Omega p\nabla\cdot\mathbf{v}\, d\Omega = \int_\Omega \mathbf{f}\cdot\mathbf{v}\, d\Omega \quad \forall\mathbf{v} \in \mathbf{H}_0^1(\Omega),\\ &\int_\Omega [\nabla\phi - (\mathbf{u}\times\mathbf{B})]\cdot(\nabla\psi)\, d\Omega = \int_\Gamma g\psi\, d\Gamma \quad \forall v \in \tilde{H}^1(\Omega), \qquad (2.4)\end{aligned}$$

and

$$\int_\Omega q\,\nabla\cdot\mathbf{u}\, d\Omega = 0 \quad \forall q \in L_0^2(\Omega). \qquad (2.5)$$

Here the colon notation stands for the scalar product on $\mathbb{R}^{d\times d}$.

The precise mathematical statement of the optimal control problem (1.10) can now be given as

$$\begin{aligned}&\text{seek a } (\mathbf{u}, p, \phi, g) \in \mathbf{H}_0^1(\Omega)\times L_0^2(\Omega)\\ &\quad \times\tilde{H}^1(\Omega)\times L^2(\Gamma) \text{ such that}\\ &\mathscr{I}(\mathbf{u}, p, \phi, g) \text{ is minimized subject}\\ &\quad \text{to the constraints (2.3)–(2.5).}\end{aligned} \qquad (2.6)$$

Using the Lagrange multiplier principles we may turn the constrained optimization problem (2.6) into an unconstrained one. For general mathematical theories of Lagrange multiplier principles, see, e.g., [11]. The rigorous

justification of the use of Lagrange multiplier rules for the problems studied in this paper will be presented elsewhere; some related results can be found in [4–5]. To make the abstract theories in optimal control more amenable to the derivation of an optimality system of equations, we introduce the following formal procedure: we set $\mathscr{X} = \mathbf{H}_0^1(\Omega) \times L_0^2(\Omega) \times \tilde{H}^1(\Omega) \times L^2(\Gamma) \times \mathbf{H}_0^1(\Omega) \times L_0^2(\Omega) \times \tilde{H}^1(\Omega)$ (i.e., the appropriate spaces for the variational formulation of the constraint equations) and define the Lagrangian functional

$$\begin{aligned}\mathscr{L}(\mathbf{u}, p, \phi, g, \boldsymbol{\mu}, \tau, s) &= \mathscr{F}(\mathbf{u}, p, \phi) + \frac{\delta}{2}\int_\Gamma g^2\, d\Gamma \\ &- \frac{1}{M^2}\int_\Omega \nabla\mathbf{u} : \nabla\mathbf{v}\, d\Omega + \int_\Omega [\nabla\phi - (\mathbf{u}\times\mathbf{B})]\cdot(\boldsymbol{\mu}\times\mathbf{B})\, d\Omega \\ &- \frac{1}{N}\int_\Omega (\mathbf{u}\cdot\nabla)\mathbf{u}\cdot\boldsymbol{\mu}\, d\Omega + \int_\Omega p\nabla\cdot\boldsymbol{\mu}\, d\Omega + \int_\Omega \mathbf{f}\cdot\boldsymbol{\mu}\, d\Omega \\ &- \int_\Omega [\nabla\phi - (\mathbf{u}\times\mathbf{B})]\cdot(\nabla s)\ d\Omega + \int_\Gamma gs\, d\Gamma \\ &+ \int_\Omega \tau\nabla\cdot\mathbf{u}\, d\Omega \quad \forall(\mathbf{u}, p, \phi, g, \boldsymbol{\mu}, \tau, s) \in \mathscr{X}. \end{aligned} \tag{2.7}$$

Note that the Lagrangian is obtained by the cost functional subtracting the variational form of the constraint equations tested against the multipliers $(\boldsymbol{\mu}, \tau, s)$ (which are also termed the adjoint state variables). An optimality system of equations that an optimum must satisfy is derived by taking variations with respect to every variable in the Lagrangian. By taking variations with respect to $\mathbf{u}$, p, and ϕ, we obtain

$$\begin{aligned}&\frac{1}{M^2}\int_\Omega \nabla\boldsymbol{\mu} : \nabla\mathbf{w}\, d\Omega + \int_\Omega (\mathbf{w}\times\mathbf{B})\cdot(\boldsymbol{\mu}\times\mathbf{B})\, d\Omega \\ &\quad + \frac{1}{N}\int_\Omega (\mathbf{u}\cdot\nabla)\mathbf{w}\cdot\boldsymbol{\mu}\, d\Omega \\ &\quad + \frac{1}{N}\int_\Omega (\mathbf{w}\cdot\nabla)\mathbf{u}\cdot\boldsymbol{\mu}\, d\Omega - \int_\Omega \tau\nabla\cdot\mathbf{w}\, d\Omega \\ &\quad = \langle \mathscr{F}_{\mathbf{u}}(\mathbf{u}, p, \phi), \mathbf{w}\rangle \quad \forall\mathbf{w} \in \mathbf{H}_0^1(\Omega), \\ &\int_\Omega [\nabla s - (\boldsymbol{\mu}\times\mathbf{B})]\cdot(\nabla r)\, d\Omega = \langle \mathscr{F}_\phi(\mathbf{u}, p, \phi), r\rangle \quad \forall r \in \tilde{H}^1(\Omega), \end{aligned} \tag{2.8}$$

and

$$\int_\Omega \sigma\nabla\cdot\boldsymbol{\mu}\, d\Omega = \langle \mathscr{F}_p(\mathbf{u}, p, \phi), \sigma\rangle \quad \forall\sigma \in L_0^2(\Omega), \tag{2.9}$$

where $\mathscr{F}_{\mathbf{u}}$, $\mathscr{F}_\phi$, and $\mathscr{F}_p$ are the derivatives of the functional with respect to its three arguments, respectively. By taking variations with respect to $\boldsymbol{\mu}$, τ, and s, we recover the constraint equations (2.3)–(2.5). By taking variation with respect to g we obtain

$$\int_\Gamma (\delta g z + z s)\, d\Gamma = 0 \quad \forall z \in L^2(\Gamma); \quad \text{i.e., } g = -\frac{1}{\delta}s.$$

This last equation enables us to eliminate the control g in (2.4). Thus (2.3)–(2.5) can be replaced by

$$\begin{aligned}&\frac{1}{M^2}\int_\Omega \nabla\mathbf{u} : \nabla\mathbf{v}\, d\Omega - \int_\Omega [\nabla\phi - (\mathbf{u}\times\mathbf{B})]\cdot(\mathbf{v}\times\mathbf{B})\, d\Omega \\ &\quad + \frac{1}{N}\int_\Omega (\mathbf{u}\cdot\nabla)\mathbf{u}\cdot\mathbf{v}\, d\Omega - \int_\Omega p\Omega\cdot\mathbf{v}\, d\Omega \\ &\quad = \int_\Omega \mathbf{f}\cdot\mathbf{v}\, d\Omega \quad \forall\mathbf{v} \in \mathbf{H}_0^1(\Omega), \end{aligned} \tag{2.11}$$

$$\int_\Omega [\nabla\phi - (\mathbf{u}\times\mathbf{B})]\cdot(\nabla\psi)\, d\Omega + \frac{1}{\delta}\int_\Omega s\psi\, d\Gamma = 0 \quad \forall\psi \in \tilde{H}^1(\Omega), \tag{2.12}$$

and

$$\int_\Omega q\nabla\cdot\mathbf{u}\, d\Omega = 0 \quad \forall q \in L_0^2(\Omega). \tag{2.13}$$

Equations (2.8)–(2.13) form an optimality system of equations that an optimal solution must satisfy. We will compute optimal solutions by solving this system of equations.

3. FINITE ELEMENT APPROXIMATIONS

A finite element discretization of the optimality system (2.8)–(2.13) is defined in the usual manner. First, one chooses families of finite dimensional subspaces $X^h \subset H^1(\Omega)$ and $S^h \subset L^2(\Omega)$. These families are parameterized by a parameter h that tends to zero; commonly, h is chosen to be some measure of the grid size. These finite dimensional function spaces are defined on an approximate domain Ω^h. For simplicity we will state our results in this section by assuming $\Omega^h = \Omega$, which is the case when Ω is a convex polygon in two dimensions or a convex polyhedral in three dimensions. We set $\tilde{X}^h = X^h \cap L_0^2(\Omega)$, $\mathbf{X}^h = [X^h]^d$, $\mathbf{X}_0^h = \mathbf{X}^h \cap \mathbf{H}_0^1(\Omega)$, and $S_0^h = S^h \cap L_0^2(\Omega)$. We assume that as $h \to 0$,

$$\inf_{\mathbf{v}^h \in \mathbf{X}_0^h} \|\mathbf{v} - \mathbf{v}^h\|_1 \to 0 \quad \forall\mathbf{v} \in \mathbf{H}_0^1(\Omega),$$

$$\inf_{v^h \in \tilde{X}^h} \|v - v^h\|_1 \to 0 \quad \forall v \in \tilde{H}^1(\Omega),$$

$$\inf_{q^h \in S_0^h} \|q - q^h\|_0 \to 0 \quad \forall q \in L_0^2(\Omega).$$

Here we may choose any pair of subspaces X^h and S^h such

that $\mathbf{X}_0^h$ and S_0^h can be used for finding finite element approximations of solutions of the Navier–Stokes equations. Thus, we make the following standard assumptions, which are exactly those employed in well-known finite element methods for the Navier–Stokes equations. First, we have the approximation properties: there exist an integer k and a constant C, independent of h, $\mathbf{v}$, v, and q, such that

$$\inf_{\mathbf{v}^h \in \mathbf{X}_0^h} \|\mathbf{v} - \mathbf{v}^h\|_1 \le Ch^m \|\mathbf{v}\|_{m+1}$$

$$\forall \mathbf{v} \in \mathbf{H}^{m+1}(\Omega) \cap \mathbf{H}_0^1(\Omega), 1 \le m \le k, \quad (3.1)$$

$$\inf_{v^h \in \tilde{X}^h} \|v - v^h\|_1 \le Ch^m \|v\|_{m+1}$$

$$\forall v \in H^{m+1}(\Omega) \cap L_0^2(\Omega), 1 \le m \le k, \quad (3.2)$$

$$\inf_{q^h \in S_0^h} \|q - q^h\|_0 \le Ch^m \|q\|_m$$

$$\forall q \in H^m(\Omega) \cap L_0^2(\Omega), 1 \le m \le k. \quad (3.3)$$

Next, we assume the *inf–sup condition,* or *Ladyzhenskaya–Babuska–Brezzi condition:* there exists a constant C, independent of h, such that

$$\inf_{0 \ne q^h \in S_0^h} \sup_{0 \ne \mathbf{v}^h \in \mathbf{X}_0^h} \frac{-\int_\Omega q^h \nabla \cdot \mathbf{v}^h \, d\Omega}{\|\mathbf{v}^h\|_1 \, \|q^h\|_0} \ge C. \quad (3.4)$$

This condition assures the stability of finite element discretizations of the Navier–Stokes equations. It also assures the stability of the approximation of the constraint equations (2.3)–(2.5) and the optimality system (2.8)–(2.13). For thorough discussions of the approximation properties (3.1)–(3.3) and the stability condition (3.4), see, e.g., [2] or [3]. These references may also be consulted for a catalog of finite element subspaces that meet the requirements of (3.1)–(3.4).

Once the approximating subspaces have been chosen, we seek $\mathbf{u}^h \in \mathbf{X}_0^h$, $p^h \in S_0^h$, $\phi^h \in \tilde{X}^h$, $\boldsymbol{\mu}^h \in \mathbf{X}_0^h$, $\tau^h \in S_0^h$, and $s^h \in \tilde{X}^h$ such that

$$\frac{1}{M^2}\int_\Omega \nabla \mathbf{u}^h : \nabla \mathbf{v}^h \, d\Omega - \int_\Omega [\nabla \phi^h - (\mathbf{u}^h \times \mathbf{B})] \cdot (\mathbf{v}^h \times \mathbf{B}) \, d\Omega$$

$$+ \frac{1}{N}\int_\Omega (\mathbf{u}^h \cdot \nabla)\mathbf{u}^h \cdot \mathbf{v}^h \, d\Omega$$

$$- \int_\Omega p^h \nabla \cdot \mathbf{v}^h \, d\Omega = \int_\Omega \mathbf{f} \cdot \mathbf{v}^h \, d\Omega \quad \forall \mathbf{v}^h \in \mathbf{X}_0^h, \quad (3.5)$$

$$\int_\Omega [\nabla \phi^h - (\mathbf{u}^h \times \mathbf{B})] \cdot (\nabla \psi^h) \, d\Omega + \frac{1}{\delta}\int_\Gamma s^h \psi^h \, d\Gamma = 0$$

$$\forall \psi^h \in \tilde{X}^h, \quad (3.6)$$

$$\int_\Omega q^h \nabla \cdot \mathbf{u}^h \, d\Omega = 0 \quad \forall q^h \in S_0^h, \quad (3.7)$$

$$\frac{1}{M^2}\int_\Omega \nabla \boldsymbol{\mu}^h : \nabla \mathbf{w}^h \, d\Omega + \int_\Omega (\mathbf{w}^h \times \mathbf{B}) \cdot (\boldsymbol{\mu}^h \times \mathbf{B}) \, d\Omega$$

$$+ \frac{1}{N}\int_\Omega (\mathbf{u}^h \cdot \nabla)\mathbf{w}^h \cdot \boldsymbol{\mu}^h \, d\Omega \quad (3.8)$$

$$+ \frac{1}{N}\int_\Omega (\mathbf{w}^h \cdot \nabla)\mathbf{u}^h \cdot \boldsymbol{\mu}^h \, d\Omega - \int_\Omega \tau^h \nabla \cdot \mathbf{w}^h \, d\Omega$$

$$= \langle \mathscr{F}_{\mathbf{u}}(\mathbf{u}^h, p^h, \phi^h), \mathbf{w}^h \rangle \quad \forall \mathbf{w}^h \in \mathbf{X}_0^h,$$

$$\int_\Omega [\nabla s^h - (\mathbf{u}^h \times \mathbf{B})] \cdot (\nabla r^h) \, d\Omega = \langle \mathscr{F}_\phi(\mathbf{u}^h, p^h, \phi^h), r^h \rangle$$

$$\forall r^h \in \tilde{X}^h, \quad (3.9)$$

and

$$\int_\Omega \sigma^h \nabla \cdot \boldsymbol{\mu}^h \, d\Omega = \langle \mathscr{F}_p(\mathbf{u}^h, p^h, \phi^h), \sigma^h \rangle \quad \forall \sigma^h \in S_0^h. \quad (3.10)$$

From a computational standpoint, this is a formidable system. In three dimensions, we have a coupled system involving *ten* unknown discrete scalar fields. Therefore, how one solves this system is a rather important question.

4. SOLUTION METHODS FOR THE DISCRETE OPTIMALITY SYSTEM OF EQUATIONS

We will present two methods for solving the discrete optimality system of Eqs. (3.5)–(3.10). The first one is Newton's method for the entire system; the second one is an iterative method which uncouples the computation of (3.5)–(3.7) and the computation of (3.8)–(3.10) at each iteration (the second method is in essence equivalent to a gradient method in minimization.)

4.1. *Newton's Method*

For notational convenience, we will use ($\mathbf{U}$, P, Φ, $\mathbf{M}$, T, S) to denote ($\mathbf{u}^h$, p^h, ϕ^h, $\boldsymbol{\mu}^h$, τ^h, s^h). We will only give Newton's method for the special case $\mathscr{F}(\mathbf{u}, p, \phi) = \mathscr{F}(\mathbf{u})$. General cases can be treated similarly. Thus Newton's method for solving the discrete optimality system (3.5)–(3.10) is

1. Choose an initial guess ($\mathbf{U}^{(0)}$, $P^{(0)}$, $\Phi^{(0)}$, $\mathbf{M}^{(0)}$, $T^{(0)}$, $S^{(0)}$);

2. For $n = 1, 2, \ldots$ compute ($\mathbf{U}^{(n)}$, $P^{(n)}$, $\Phi^{(n)}$, $\mathbf{M}^{(n)}$, $T^{(n)}$, $S^{(n)}$) from the following discrete system of equations:

$$\frac{1}{M^2}\int_\Omega \nabla \mathbf{U}^{(n)} : \nabla \mathbf{v}^h \, d\Omega - \int_\Omega [\nabla \Phi^{(n)} - (\mathbf{U}^{(n)} \times \mathbf{B})] \cdot (\mathbf{v}^h \times \mathbf{B}) \, d\Omega$$

$$+ \frac{1}{N}\int_\Omega (\mathbf{U}^{(n-1)} \cdot \nabla)\mathbf{U}^{(n)} \cdot \mathbf{v}^h \, d\Omega$$

$$+ \frac{1}{N}\int_\Omega (\mathbf{U}^{(n)} \cdot \nabla)\mathbf{U}^{(n-1)} \cdot \mathbf{v}^h \, d\Omega - \int_\Omega P^{(n)} \nabla \cdot \mathbf{v}^h \, d\Omega$$

$$= \int_\Omega \mathbf{f} \cdot \mathbf{v}^h \, d\Omega + \int_\Omega (\mathbf{U}^{(n-1)} \cdot \nabla)\mathbf{U}^{(n-1)} \cdot \mathbf{v}^h \, d\Omega \quad \forall \mathbf{v}^h \in \mathbf{X}_0^h, \quad (4.1)$$

$$\int_\Omega [\nabla \Phi^{(n)} - (\mathbf{U}^{(n)} \times \mathbf{B})] \cdot (\nabla \psi^h)\, d\Omega + \frac{1}{\delta} \int_\Gamma S^{(n)} \psi^h\, d\Gamma = 0 \quad \forall \psi^h \in \tilde{X}^h, \quad (4.2)$$

$$\int_\Omega q^h \nabla \cdot \mathbf{U}^{(n)}\, d\Omega = 0 \quad \forall q^h \in S_0^h, \quad (4.3)$$

$$\begin{aligned} &\frac{1}{M^2} \int_\Omega \nabla \mathbf{M}^{(n)} : \nabla \mathbf{w}^h\, d\Omega + \int_\Omega (\mathbf{w}^h \times \mathbf{B}) \cdot (\mathbf{M}^{(n)} \times \mathbf{B})\, d\Omega \\ &\quad + \frac{1}{N} \int_\Omega (\mathbf{U}^{(n)} \cdot \nabla) \mathbf{w}^h \cdot \mathbf{M}^{(n-1)}\, d\Omega \\ &\quad + \frac{1}{N} \int_\Omega (\mathbf{U}^{(n-1)} \cdot \nabla) \mathbf{w}^h \cdot \mathbf{M}^{(n)}\, d\Omega \\ &\quad + \frac{1}{N} \int_\Omega (\mathbf{w}^h \cdot \nabla) \mathbf{U}^{(n-1)} \cdot \mathbf{M}^{(n)}\, d\Omega \\ &\quad + \frac{1}{N} \int_\Omega (\mathbf{w}^h \cdot \nabla) \mathbf{U}^{(n)} \cdot \mathbf{M}^{(n-1)}\, d\Omega - \int_\Omega T^{(n)} \nabla \cdot \mathbf{w}^h\, d\Omega \\ &\quad - \langle \mathscr{T}_{\mathbf{uu}}(\mathbf{U}^{(n-1)}) \mathbf{U}^{(n)}, \mathbf{w}^h \rangle \\ &= \langle \mathscr{T}_{\mathbf{u}}(\mathbf{U}^{(n-1)}), \mathbf{w}^h \rangle - \langle \mathscr{T}_{\mathbf{uu}}(\mathbf{U}^{(n-1)}) \mathbf{U}^{(n-1)}, \mathbf{w}^h \rangle \\ &\quad + \frac{1}{N} \int_\Omega (\mathbf{U}^{(n-1)} \cdot \nabla) \mathbf{w}^h \cdot \mathbf{M}^{(n-1)}\, d\Omega \\ &\quad + \frac{1}{N} \int_\Omega (\mathbf{w}^h \cdot \nabla) \mathbf{U}^{(n-1)} \cdot \mathbf{M}^{(n-1)}\, d\Omega \quad \forall \mathbf{w}^h \in \mathbf{X}_0^h, \end{aligned} \quad (4.4)$$

$$\int_\Omega [\nabla S^{(n)} - (\mathbf{M}^{(n)} \times \mathbf{B})] \cdot (\nabla r^h)\, d\Omega = 0 \quad \forall r^h \in \tilde{X}^h \quad (4.5)$$

and

$$\int_\Omega \sigma^h \nabla \cdot \mathbf{M}^{(n)}\, d\Omega = 0 \quad \forall \sigma^h \in S_0^h. \quad (4.6)$$

Under suitable assumptions, Newton's method converges at a quadratic rate to the finite element solution $(\mathbf{U}, P, \Phi, \mathbf{M}, T, S)$. The convergence properties will be analyzed elsewhere. Quadratic convergence of Newton's method is valid within a contraction ball. In practice we normally first perform a few simple iterations and then switch to Newton's method. The simple iterations are defined by replacing equations (4.1) and (4.4) in Newton's iterations by

$$\begin{aligned} &\frac{1}{M^2} \int_\Omega \nabla \mathbf{U}^{(n)} : \nabla \mathbf{v}^h\, d\Omega - \int_\Omega [\nabla \Phi^{(n)} - (\mathbf{U}^{(n)} \times \mathbf{B})] \cdot (\mathbf{v}^h \times \mathbf{B})\, d\Omega \\ &\quad + \frac{1}{N} \int_\Omega (\mathbf{U}^{(n-1)} \cdot \nabla) \mathbf{U}^{(n)} \cdot \mathbf{v}^h\, d\Omega \\ &\quad - \int_\Omega P^{(n)} \nabla \cdot \mathbf{v}^h\, d\Omega = \int_\Omega \mathbf{f} \cdot \mathbf{v}^h\, d\Omega \quad \forall \mathbf{v}^h \in \mathbf{X}_0^h \end{aligned}$$

and

$$\begin{aligned} &\frac{1}{M^2} \int_\Omega \nabla \mathbf{M}^{(n)} : \nabla \mathbf{w}^h\, d\Omega + \int_\Omega (\mathbf{w}^h \times \mathbf{B}) \cdot (\mathbf{M}^{(n)} \times \mathbf{B})\, d\Omega \\ &\quad + \frac{1}{N} \int_\Omega (\mathbf{U}^{(n-1)} \cdot \nabla) \mathbf{w}^h \cdot \mathbf{M}^{(n)}\, d\Omega \\ &\quad + \frac{1}{N} \int_\Omega (\mathbf{w}^h \cdot \nabla) \mathbf{U}^{(n-1)} \cdot \mathbf{M}^{(n)}\, d\Omega - \int_\Omega T^{(n)} \nabla \cdot \mathbf{w}^h\, d\Omega \\ &= \langle \mathscr{T}_{\mathbf{u}}(\mathbf{U}^{(n-1)}), \mathbf{w}^h \rangle, \mathbf{w}^h \rangle \quad \forall \mathbf{w}^h \in \mathbf{X}_0^h. \end{aligned}$$

For flow-field matching problems, we use the desired field as initial data for the corresponding unknown field. This choice has proven to produce faster convergence, compared with an arbitrary choice of initial data.

4.2. *An Iterative Method*

We now discuss an iterative method that uncouples the solution of the constraint equations (2.11)–(2.13) from the adjoint equations (2.8)–(2.10).

1. Choose $(\mathbf{U}^{(0)}, P^{(0)}, \mathbf{\Phi}^{(0)})$;
2. For $n = 1, 2, 3, \ldots$, compute $(\mathbf{M}^{(n)}, T^{(n)}, S^{(n)})$ from

$$\begin{aligned} &\frac{1}{M^2} \int_\Omega \nabla \mathbf{M}^{(n)} : \nabla \mathbf{w}^h\, d\Omega + \int_\Omega (\mathbf{w}^h \times \mathbf{B}) \cdot (\mathbf{M}^{(n)} \times \mathbf{B})\, d\Omega \\ &\quad + \frac{1}{N} \int_\Omega (\mathbf{U}^{(n-1)} \cdot \nabla) \mathbf{w}^h \cdot \mathbf{M}^{(n)}\, d\Omega \\ &\quad + \frac{1}{N} \int_\Omega (\mathbf{w}^h \cdot \nabla) \mathbf{U}^{(n-1)} \cdot \mathbf{M}^{(n)}\, d\Omega - \int_\Omega T^{(n)} \nabla \cdot \mathbf{w}^h\, d\Omega \\ &= \langle \mathscr{T}_{\mathbf{u}}(\mathbf{U}^{(n-1)}), P^{(n-1)}, \Phi^{(n-1)}), \mathbf{w}^h \rangle, \quad \forall \mathbf{w}^h \in \mathbf{X}_0^h. \end{aligned} \quad (4.7)$$

$$\begin{aligned} &\int_\Omega [\nabla S^{(n)} - (\mathbf{M}^{(n)} \times \mathbf{B})] \cdot (\nabla r^h)\, d\Omega \\ &\quad = \langle \mathscr{T}_\phi(\mathbf{U}^{(n-1)}, P^{(n-1)}, \Phi^{(n-1)}), r^h \rangle \quad \forall r^h \in \tilde{X}^h, \end{aligned} \quad (4.8)$$

and

$$\begin{aligned} &\int_\Omega \sigma^h \nabla \cdot \mathbf{M}^{(n)}\, d\Omega \\ &\quad = \langle \mathscr{T}_p(\mathbf{U}^{(n-1)}, P^{(n-1)}, \Phi^{(n-1)}), \sigma^h \rangle \quad \forall \sigma^h \in S_0^h; \end{aligned} \quad (4.9)$$

and compute $(\mathbf{U}^{(n)}, P^{(n)}, \Phi^{(n)}$ from

$$\begin{aligned} &\frac{1}{M^2} \int_\Omega \nabla \mathbf{U}^{(n)} : \nabla \mathbf{v}^h\, d\Omega - \int_\Omega [\nabla \Phi^{(n)} - (\mathbf{U}^{(n)} \times \mathbf{B})] \\ &\qquad \cdot (\mathbf{v}^h \times \mathbf{B})\, d\Omega + \frac{1}{N} \int_\Omega (\mathbf{U}^{(n)} \cdot \nabla) \mathbf{U}^{(n)} \cdot \mathbf{v}^h\, d\Omega \\ &\qquad - \int_\Omega P^{(n)} \nabla \cdot \mathbf{v}^h\, d\Omega \\ &\quad = \int_\Omega \mathbf{f} \cdot \mathbf{v}^h\, d\Omega \quad \forall \mathbf{v}^h \in \mathbf{X}_0^h, \end{aligned} \quad (4.10)$$

$$\int_\Omega [\nabla\Phi^{(n)} - (\mathbf{U}^{(n)} \times \mathbf{B})] \cdot (\nabla\psi^h)\, d\Omega + \frac{1}{\delta}\int_\Gamma S^{(n)}\Psi^h\, d\Gamma = 0 \quad \forall\psi^h \in \tilde{X}^h, \tag{4.11}$$

$$\int_\Omega q^h \nabla\cdot \mathbf{U}^{(n)} d\Omega = 0 \quad \forall q^h \in S_0^h. \tag{4.12}$$

Formally this method is equivalent to a gradient method with unit step-length for minimizing the functional of g:

$$\tilde{\mathscr{J}}(g) \equiv \mathscr{J}(\mathbf{U}(g), P(g), \Phi(g), g).$$

Under suitable assumptions, most notably for large parameters ε and δ in the functional, the sequence $(\mathbf{U}^{(n)}, P^{(n)}, \Phi^{(n)}, \mathbf{M}^{(n)}, T^{(n)}, S^{(n)})$ converges. We may modify this iterative method to a variable step-length gradient method which has better convergence properties.

The main advantage of this method over Newton's method is that at each iteration we are dealing with a smaller size nonlinear system which requires less computer memory in computation. In our experience, the computing times for Newton's method is generally less than this iterative method—e.g., for the inverted backward facing step example presented in Section 6, the CPU time on a SUN SPARC20 for Newton's method was 11 s and the CPU time for the iterative method was 25 s (the accuracy in both cases was 10^{-6}). Thus our conclusion about the choice of the two methods is that, whenever the RAM of the computer is large enough (i.e., no RAM swapping), then Newton's method is preferable.

5. SOME MATHEMATICAL RESULTS CONCERNING THE OPTIMALITY SYSTEM OF EQUATIONS AND FINITE ELEMENT APPROXIMATIONS

For completeness, we summarize without proof the relevant mathematical results for the constrained minimization problem and the error estimation results for the finite element approximation. The rigorous mathematical proofs will be presented elsewhere.

First, the system of state equations (2.3)–(2.5) is a well-posed; i.e., there exists a $(\mathbf{u}, p, \phi)$ satisfying (2.3)–(2.5); furthermore, any solution $(\mathbf{u}, p, \phi)$ of (2.3)–(2.5) is bounded by the data.

Second, there exists an optimal solution $(\mathbf{u}, \phi, p, g)$ for the constrained minimization problem (2.6). In most cases, the optimal solution is unique.

Third, there exist a triplet Lagrange multiplier $(\boldsymbol{\mu}, \tau, s)$ such that the adjoint state equations (2.8)–(2.10) is satisfied. This in turn justifies that the optimality system of Eqs. (2.8)–(2.13), which was formally derived by using the Lagrange multiplier principles, possesses a solution $(\mathbf{u}, \phi, p, \boldsymbol{\mu}, \tau, s)$. Thus we are justified to find optimal control solutions by solving the optimality system of equations.

Fourth, concerning the finite element approximations of solutions of the optimality system of equations, we may prove that there exists a finite element solution $(\mathbf{u}^h, \phi^h, p^h, \boldsymbol{\mu}^h, \tau^h, s^h) \in \mathbf{X}_0^h \times S_0^h \times \tilde{X}^h \times \mathbf{X}_0^h \times S_0^h \times \tilde{X}^h$ for (3.5)–(3.10); the finite element solution $(\mathbf{u}^h, \phi^h, p^h, \boldsymbol{\mu}^h, \tau^h, s^h)$ converges to the exact solution $(\mathbf{u}, \phi, p, \boldsymbol{\mu}, \tau, s)$; and the following error estimate holds:

$$\|\mathbf{u} - \mathbf{u}^h\|_1 + \|p - p^h\|_0 + \|\phi - \phi^h\|_1 + \|\boldsymbol{\mu} - \boldsymbol{\mu}^h\|_1 + \|\tau - \tau^h\|_0 + \|s - s^h\|_1 \le Ch^m.$$

An approximate control can be computed by $g^h = -(1/\delta)s^h$. Consequently, the approximate control g^h converges to the exact control g and the estimate $\|g - g^h\|_{0,\Gamma} \le Ch^m$ holds.

6. COMPUTATIONAL EXAMPLES

In this section, we report some computational examples that serve to illustrate the effectiveness and practicality of optimal control techniques in electrically conducting fluids. First, we treat the problem of steering the velocity field to a desired one. The second example deals with minimization of the potential gradient throughout the domain. In the third example, we consider the problem of matching the electric potential to a desired one. In the final example we attempt to minimize the vorticity in an inverted backward facing step channel flow. The geometrical domain in the last example is typically used in assessing CFD algorithms.

All computations are done with the following choice of finite element spaces defined over the same triangulation of the domain $\Omega = \bigcup K$: continuous piecewise quadratic polynomials for both components of the velocity $\mathbf{u}^h$ and adjoint velocity $\boldsymbol{\mu}^h$; continuous piecewise quadratic polynomials for the potential ϕ^h and the adjoint potential s^h; continuous piecewise linear polynomials for the pressure p^h and adjoint pressure τ^h. On each triangle, the degrees of freedom for quadratic elements are the function values at the vertices and midpoints of each edge; the degrees of freedom for linear elements are the function values at the vertices. Using standard finite element notations and those introduced in Section 3, we have that

$$\begin{aligned} X^h &= \{v \in C^0(\overline{\Omega}) : v|_K \in P_2(K), \text{ on each element } K\},\\ \mathbf{X}^h &= \{\mathbf{v} = (v_1, v_2)^{\mathrm{T}} \in \mathbf{C}^0(\overline{\Omega}) : v_i \in X^h, i = 1, 2\},\\ S^h &= \{r \in C^0(\overline{\Omega}) : r|_K \in P_1(K), \text{ on each element } K\}, \end{aligned}$$

Under these choices of finite element spaces, the velocity–pressure pair and the adjoint velocity–adjoint pressure pair are approximated by the Taylor–Hood element pair [10] which has been shown to satisfy the div-stability condi-

tion (3.4). Approximation properties (3.1)–(3.3) hold with $k = 1$.

6.1. *Velocity Field Matching*

The first case we consider is the problem of matching the velocity field with a desired one by finding an appropriate boundary current density g, i.e., minimizing (1.6) subject to (2.3)–(2.5).

The optimality system of equations are given by (2.8)–(2.13) with

$$\langle \mathscr{T}_{\mathbf{u}}(\mathbf{u}, p, \phi), \mathbf{w} \rangle = \frac{1}{\varepsilon} \int_{\Omega} (\mathbf{u} - \mathbf{u}_d) \cdot \mathbf{w} \, d\Omega$$

and

$$\langle \mathscr{T}_p(\mathbf{u}, p, \phi), \sigma \rangle = \langle \mathscr{T}_\phi(\mathbf{u}, p, \phi), r \rangle = 0.$$

The corresponding system of partial differential equations for (2.8)–(2.13) is given by (1.1)–(1.4),

$$\frac{\partial \phi}{\partial n} = -\frac{1}{\delta} s \quad \text{on } \Gamma,$$

$$-\frac{1}{M^2} \Delta \boldsymbol{\mu} + \frac{1}{N} \boldsymbol{\mu} \cdot (\nabla \mathbf{u})^{\mathrm{T}} - \frac{1}{N} (\mathbf{u} \cdot \nabla) \boldsymbol{\mu} + \nabla \tau - \mathbf{B} \times (\nabla s)$$

$$- (\boldsymbol{\mu} \times \mathbf{B}) \times \mathbf{B} - \frac{1}{\varepsilon} \mathbf{u} = -\frac{1}{\varepsilon} \mathbf{u}_d \quad \text{in } \Omega,$$

$$\nabla \cdot \boldsymbol{\mu} = 0 \quad \text{in } \Omega,$$

$$-\Delta s + \nabla \cdot (\boldsymbol{\mu} \times \mathbf{B}) = 0 \quad \text{in } \Omega,$$

$$\boldsymbol{\mu} = 0 \quad \text{on } \Gamma,$$

and

$$\frac{\partial s}{\partial n} = 0 \quad \text{on } \Gamma.$$

The data in the computational example are chosen as follows: the domain $\Omega = (0, 1) \times (0, 1)$ (i.e., the unit square), Hartmann number $M = 1$, the interaction number $N = 1$, body force $\mathbf{f} = (0, 0)^{\mathrm{T}}$, the desired velocity field

$$\mathbf{u}_d = \begin{pmatrix} \cos(2\pi y)[\cos(2\pi x) - 1] \\ \sin(2\pi x) \sin(2\pi y) \end{pmatrix},$$

and the applied magnetic field $\mathbf{B} = (0, 0, 1)^{\mathrm{T}}$. The velocity is assumed to be zero on the boundary. An optimal solution is found by solving the above system of partial differential equations, or (3.5)–(3.10), with the chosen data. The optimal velocity field $\mathbf{u}^h$ is shown in Fig. 6.1d. The optimal adjoint potential field s^h is shown in Figs. 6.1e (surface plot) and f (contour plot). The optimal control g^h can be gleaned from Fig. 6.1e and the relation $g^h = -(1/\delta)s^h$. Figure 6.1c shows the desired velocity field $\mathbf{u}_d$. It should be noted that the proper choice of the constants ε and δ in the functional plays an important role in obtaining the best velocity matching. For the computational results shown in Fig. 6.1, our choice of these two constants were $\varepsilon = 0.00001$ and $\delta = 0.01$.

For comparison we also computed an uncontrolled flow which satisfies Eqs. (1.1)–(1.4) with the same data as those chosen previously and with the additional boundary condition for the electric potential

$$\frac{\partial \phi}{\partial n} = \cos(\pi x) \cos(\pi y) \quad \text{on } \Gamma.$$

Figures 6.1a and b show the uncontrolled velocity field $\mathbf{u}_0$ and potential field ϕ_0, respectively.

All the computational results shown in Figs. 6.1 were obtained with a 10 by 10 triangulation of the unit square. A nonuniform grid with corner refinements was used. We see from the figures that optimal control does a very good job in matching the desired velocity field which has double circulations. Also, the value of the cost functional for the optimal solution is reduced by 55%, compared to the value of the cost functional for the uncontrolled solution.

6.2. *Potential Field Matching*

The second case we consider is the problem of matching the electric potential ϕ to a desired distribution ϕ_d; i.e., we minimize functional (1.7) subject to (2.3)–(2.5).

The optimality system of equations are given by (2.8)–(2.13) with

$$\langle \mathscr{T}_\phi(\mathbf{u}, p, \phi), r \rangle = \frac{1}{\varepsilon} \int_{\Omega} (\phi - \phi_d) r \, d\Omega$$

and

$$\langle \mathscr{T}_{\mathbf{u}}(\mathbf{u}, p, \phi), \mathbf{w} \rangle = \langle \mathscr{T}_p(\mathbf{u}, p, \phi), \sigma \rangle = 0.$$

The domain is chosen to be a unit square. The Hartmann number M, interaction number N, body force $\mathbf{f}$, and applied magnetic field $\mathbf{B}$ are chosen to be the same as those in Section 6.1. The desired potential field is chosen as $\phi_d = 1.5 - [(x - 0.5)^2 + (y - 0.5)^2]$. The two parameters in the functional are chosen as $\varepsilon = 0.002$ and $\delta = 0.1$.

Some numerical results for this example are reported in Figs. 6.2a–d. We give a brief description of the figures. Figures 6.2a and b are the desired potential field ϕ_d and the optimal potential field ϕ^h, respectively. Figures 6.2c and d are the contours of potential field ϕ^h and the contours of desired potential field ϕ_d, respectively.

A look at Figs. 6.2a and b reveals that the optimal potential matches well with the desired potential ϕ_d. Also, the value of the cost functional for the optimal solution is

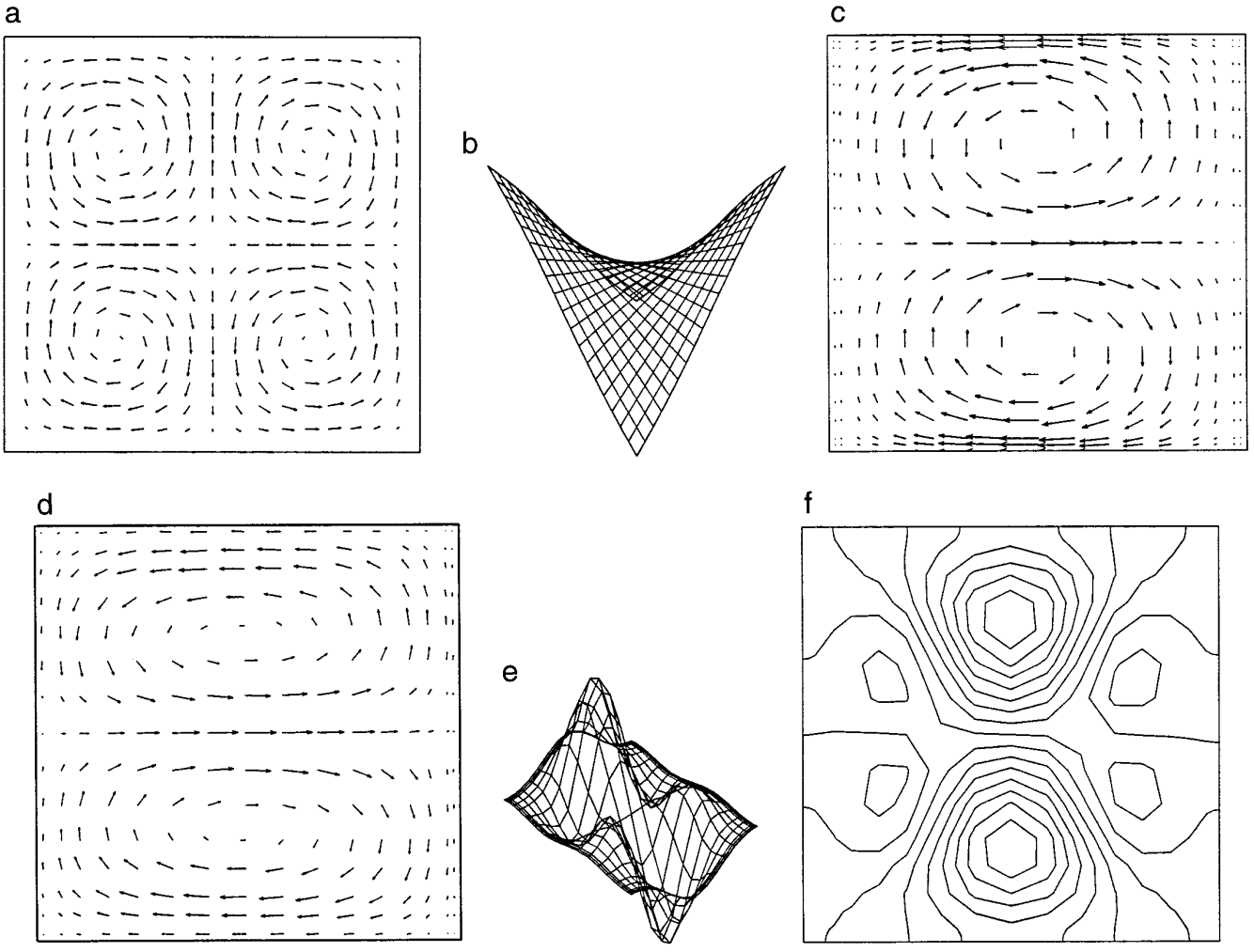

FIG. 6.1. (a) Uncontrolled velocity field $\mathbf{u}_0$; (b) uncontrolled potential field ϕ_0; (c) desired velocity field $\mathbf{u}_d$; (d) optimal control solution: velocity field $\mathbf{u}^h$; (e) optimal control solution: adjoint potential field s^h; (f) optimal control solution: contours of adjoint potential field s^h.

reduced by 90%, compared to the value of the cost functional for the uncontrolled solution.

6.3. *Potential Gradient Minimization*

The third case we consider is the problem of minimizing the electric potential gradient; i.e., we minimize functional (1.8) subject to (2.3)–(2.5). The optimality system of equations are given by (2.8)–(2.13) with

$$\langle \mathscr{T}_\phi(\mathbf{u}, p, \phi), r\rangle = \frac{1}{\varepsilon}\int_\Omega \nabla\phi\cdot\nabla r\, d\Omega$$

and

$$\langle \mathscr{T}_\mathbf{u}(\mathbf{u}, p, \phi), \mathbf{w}\rangle = \langle \mathscr{T}_p(\mathbf{u}, p, \phi), \sigma\rangle = 0.$$

The domain is chosen to be a rectangle with length 3 and height 1. The Hartmann number M, interaction number N, body force $\mathbf{f}$, and applied magnetic field $\mathbf{B}$ are chosen to be the same as in Section 6.1. The two parameters in the functional are chosen as $\varepsilon = 0.0002$ and $\delta = 1$.

Some numerical results for this example are reported in Figs. 6.3a–d. We give a brief description of the figures. Figures 6.3a and b are the uncontrolled potential field ϕ_0 and contours of potential field ϕ_0, respectively. ϕ_0 is obtained by solving (1.1)–(1.5) with $g = \cos(\pi x)\cos(\pi y)$. Figures 6.3c and d are the optimal potential field ϕ^h and the adjoint potential field s^h; those were obtained by solving (3.5)–(3.10). The optimal control g^h can be gleaned from Fig. 6.3d and the relation $g^h = -(1/\delta)s^h$.

By minimizing functional (1.8) we wish to obtain a quasi-uniform potential distribution. The numerical results (in particular, Fig. 6.3c) demonstrate that the optimal control did a very good job in achieving this objective. Also, the value of the cost functional for the optimal solution is reduced by 90%, compared to the value of the cost functional for the uncontrolled solution.

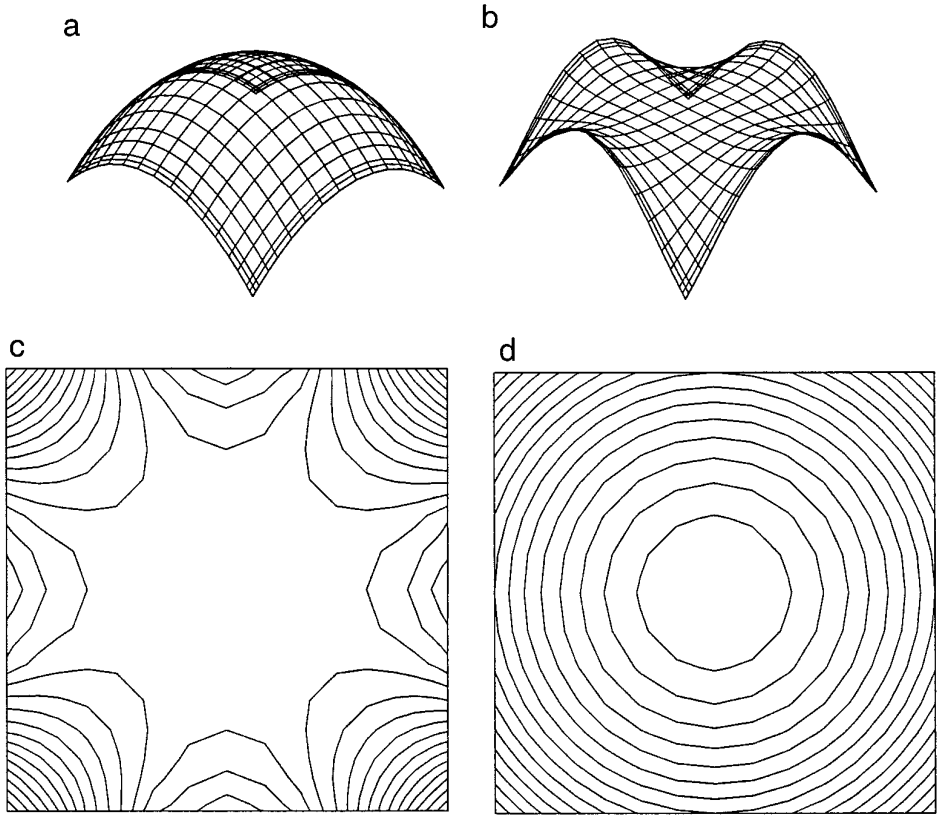

FIG. 6.2. (a) Desired potential field ϕ_d; (b) optimal control solution: potential field ϕ^h; (c) optimal control solution: contours of potential field ϕ^h; (d) contours of uncontrolled potential field ϕ_0.

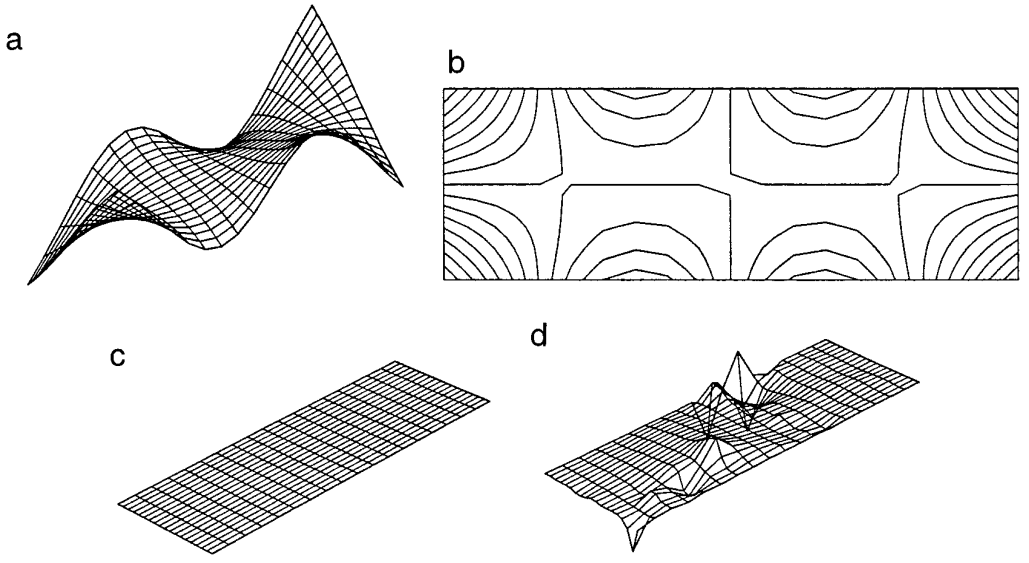

FIG. 6.3. (a) Uncontrolled potential field ϕ_0; (b) contours of uncontrolled potential field ϕ_0; (c) optimal control solution: potential field ϕ^h; (d) optimal control solution: adjoint potential field s^h.

6.4. *Vorticity Minimization*

The last problem we consider is the problem of minimizing the vorticity in a backward facing step channel flow; i.e., we minimize the functional (1.9) subject to (2.2)–(2.5). The optimality system of equations are given by (2.8)–(2.13) with

$$\langle \mathscr{T}_{\mathbf{u}}(\mathbf{u}, p, \phi), \mathbf{w} \rangle = \frac{1}{\varepsilon} \int_{\Omega} (\operatorname{curl} \mathbf{u})(\operatorname{curl} \mathbf{w})\, d\Omega$$

and

$$\langle \mathscr{T}_{\phi}(\mathbf{u}, p, \phi), r \rangle = \langle \mathscr{T}_{p}(\mathbf{u}, p, \phi), \sigma \rangle = 0.$$

The data are chosen as follows. The height of the inflow (left) boundary is 0.5 and that of the outflow (right) boundary is 1. The length of the very bottom boundary is 5 and the total horizontal length is 6. We choose the Hartmann number $M = 200$, the interaction number $N = 1$, and the applied magnetic field $\mathbf{B}$ to be the same as in Section 6.1. The two parameters in the functional are chosen as $\varepsilon = 0.01$ and $\delta = 1$. We assume the inflow and outflow velocities are parabolic profiles with

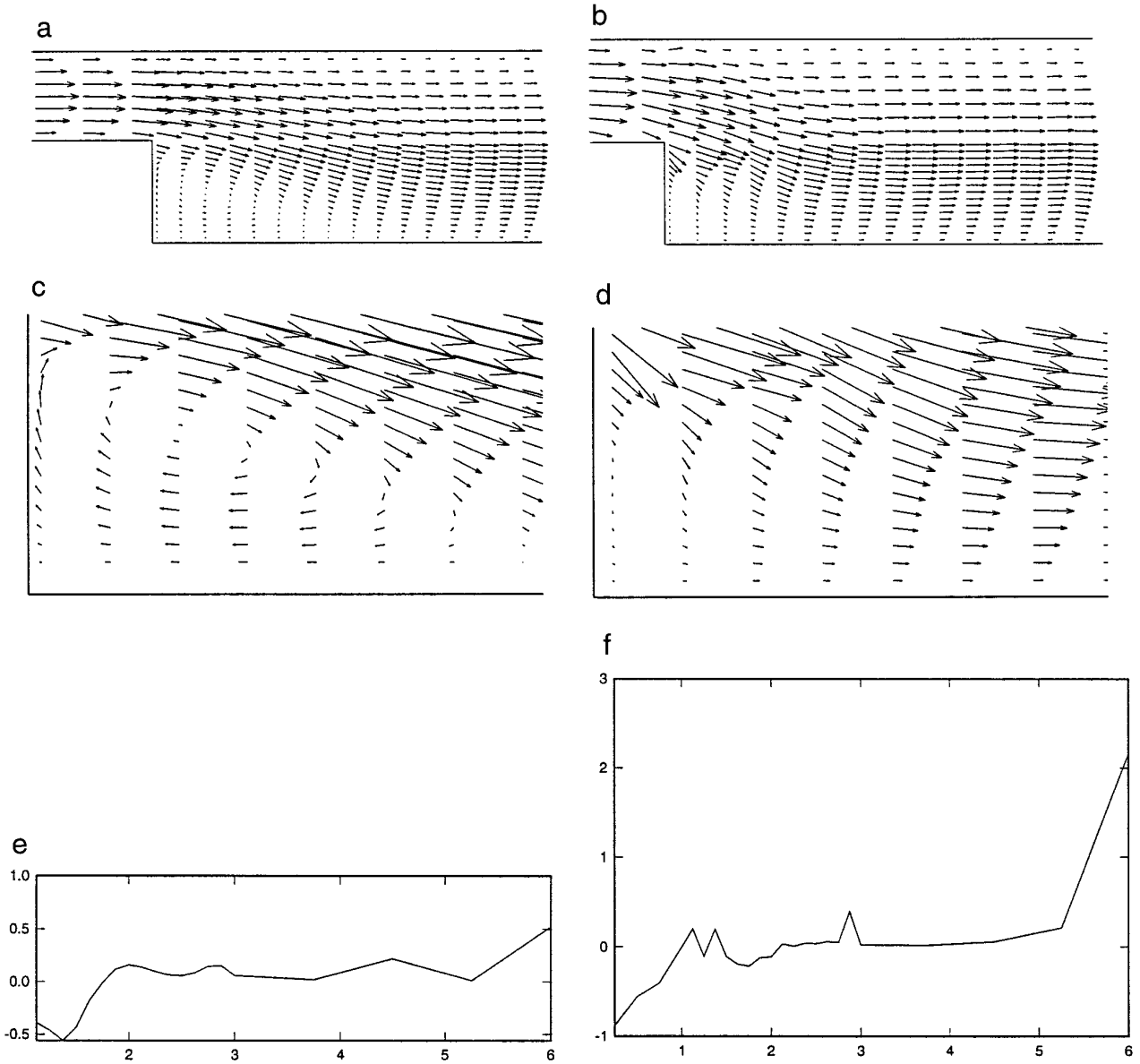

FIG. 6.4. (a) Uncontrolled velocity field $\mathbf{u}_0$; (b) optimal velocity field $\mathbf{u}^h$; (c) partial enlargement of Fig. 6.4a; (d) partial enlargement of Fig. 6.4b; (e) optimal control g^h along $y = 0$; (f) optimal control g^h along $y = 1$.

$$\mathbf{u} = \begin{pmatrix} 8(0.5 - y)(1 - y) \\ 0 \end{pmatrix} \quad \text{at the inflow (left) boundary}$$

and

$$\mathbf{u} = \begin{pmatrix} (1 - y)y \\ 0 \end{pmatrix} \quad \text{at the outflow (right) boundary;}$$

we assume $\mathbf{u} = 0$ elsewhere on the boundary. For the electric potential, we assume $\partial\phi/\partial n = 0$ at the inlet, outlet, and the very top and very bottom boundaries; elsewhere on the boundary (i.e., on the step portion) we assume $\phi = 1$. A recirculation appears at the corner region whose size increases with increasing Reynolds number. The objective is to reduce recirculation by applying control on the very top and very bottom boundaries.

For these data, the (computed) uncontrolled solution $(\mathbf{u}_0, p_0, \phi_0)$(with the boundary condition $g = 0$) is given in Fig. 6.4a (only the velocity field is shown).

Figure 6.4b gives the velocity field $\mathbf{u}^h$ of the optimal control solution. Figures 6.4c and 6.4d are the blowup of the uncontrolled and controlled flows, respectively, at the corner of the backward facing step. Figures 6.4e and 6.4f are the control distribution on the very top and very bottom boundaries.

By the minimizing functional (1.9) we wish to obtain a velocity distribution that has minimal vorticity. The numerical results (in particular, Fig. 6.4b) demonstrate that the optimal control did a very good job in achieving this objective.

7. CONCLUDING REMARKS

In this paper we studied the numerical computation of boundary optimal control problems for an electrically conducting fluid. We summarize the main points in this article as follows:

- we developed a systematic method to convert the optimal control problem into a system of equations (i.e., an optimality system of equations). The main steps involve rewriting the governing differential equations into an appropriate variational formulation, forming the Lagrangian functional in terms of this variational formulation and the cost functional, and then taking the variations of the Lagrangian functional with respect to each of its arguments;
- we proposed a direct method and an iterative method for solving the discrete optimality system of equations. Our discussions of these methods were made for finite element discretizations. Apparently, these methods are equally applicable to finite difference, collocation, or pseudo-spectral discretizations;
- in view of the fact that the computing time for the proposed Newton's method is generally less than that for the iterative method in solving the discrete optimality system of equations, we recommend that Newton's method be used whenever the computations can be done without RAM swapping; and
- we successfully performed numerical computations for some prototype examples as presented in the figures. Our work demonstrated the effectiveness of optimal control techniques in flowfield matchings and in the minimization of some physical quantities. It turns out that the appropriate choice of the parameters ε and δ plays an important role in obtaining a good matching. A rule of thumb for choosing ε and δ is that the product $(\varepsilon\delta)$ be sufficiently small.

In principle, other types of boundary controls, such as Dirichlet controls of the electrical potential or Dirichlet controls of the boundary velocity, can all be treated by the techniques used in this paper. In practical calculation, the optimality system of equations for Dirichlet controls involves one more equation defined along the boundary (see, e.g., [5]).

REFERENCES

1. J. Blum, *Numerical Simulation and Optimal Control in Plasma Physics: With Applications to Tokamaks* (Gauthier–Villars, Paris, 1989).
2. V. Girault and P.-A. Raviart, *Finite Element Methods for Navier–Stokes Equations* (Springer-Verlag, Berlin, 1986).
3. M. D. Gunzburger, *Finite Element Methods for Viscous Incompressible Flow: A Guide to Theory, Practice and Algorithm* (Academic Press, Boston, 1989).
4. L. S. Hou and A. J. Meir, *J. Appl. Math. Optim.* **32,** 143 (1995).
5. L. S. Hou and J. Peterson, *Nonlinear Anal.* **24,** 857 (1995).
6. L. S. Hou and S. S. Ravindran, Finite element approximation of optimal control problems for electrically conducting fluids, in *Proc. Sympos. Appl. Math*., Vol. 48 (Amer. Math. Soc.), Providence, RI, (1994), p. 305.
7. H. K. Moffatt, "Electrically Driven Steady Flows in Magnetohydrodynamics, in *Proceedings, 11th International Congress of Applied Mechanics, 1964*, p. 946.
8. J. Peterson, *Numer. Methods Partial Differential Equations* **4,** 57 (1988).
9. S. S. Ravindran, Ph.D. thesis, Simon Fraser University, August 1994 (unpublished).
10. C. Taylor and P. Hood, *Comput. Fluids* **1,** 73 (1973).
11. V. Tikhomirow, *Fundamental Principles of the Theory of External Problems* (Wiley, Chichester, 1982).
12. J. S. Walker, "Large Interaction Parameter Magnetohydrodynamics and Applications in Fusion Reactor Technology," in *Fluid Mechanics in Energy Conversion*, edited by J. Buchmaster (SIAM, Philadelpia, 1980).
13. N. Winowich and W. Hughes, "A Finite Element Analysis of Two-Dimensional MHD Flows," in *Liquid-Metal Flows and Magnetohydrodynamics*, edited by H. Branover, P. S. Lykoudis, and A. Yakhot (AIAA, New York, 1983).